









RESEARCH ARTICLE OPEN ACCESS

A Method to Visualize Cell Proliferation of *Arabidopsis thaliana*: A Case Study of the Root Apical Meristem

J. Irepan Reyes-Olalde^{1,2} | Miguel Tapia-Rodríguez³ | Vadim Pérez-Koldenkova⁴  | Gastón Contreras-Jiménez^{1,5}  | Paul Hernández-Herrera^{6,7}  | Gabriel Corkidi⁶  | Arturo J. Arciniega-González¹  | Maria De La Paz-Sánchez¹ | Berenice García-Ponce¹  | Adriana Garay-Arroyo¹  | Elena R. Álvarez-Buylla¹ 

¹Laboratorio de Genética Molecular, Epigenética, Desarrollo y Evolución de Plantas, Instituto de Ecología, Universidad Nacional Autónoma de México, Ciudad Universitaria, Ciudad de México, México | ²Laboratorio de Botánica, Universidad Estatal del Valle de Toluca, Ocoyoacac, Mexico | ³Unidad de Microscopía, Instituto de Investigaciones Biomédicas, Universidad Nacional Autónoma de México, Ciudad Universitaria, Ciudad de México, México | ⁴Laboratorio Nacional de Microscopía Avanzada, Centro Médico Nacional Siglo XXI-IMSS, Instituto Mexicano del Seguro Social, Ciudad de México, Mexico | ⁵Laboratorio de Microscopía y Microdissección Láser, Instituto de Ecología, Universidad Nacional Autónoma de México, Ciudad Universitaria, Ciudad de México, México | ⁶Departamento de Ingeniería Celular y Biocatálisis, Laboratorio de Imágenes y Visión por Computadora, Instituto de Biotecnología, UNAM, Cuernavaca, México | ⁷Facultad de Ciencias, Universidad Autónoma de San Luis Potosí, San Luis Potosí, México

Correspondence: Elena R. Álvarez-Buylla (eabuylla@gmail.com)

Received: 10 April 2024 | **Revised:** 12 February 2025 | **Accepted:** 3 March 2025

Funding: This work was supported by UNAM | Dirección General de Asuntos del Personal Académico, Universidad Nacional Autónoma de México (DGAPA), Universidad Nacional Autónoma de México (UNAM) (IN211721), and Consejo Nacional de Ciencia y Tecnología (CONACYT) (102959 and CF-2023-G-708).

Keywords: 5-ethynyl-2-deoxyuridine (EdU) | cell and nuclear markers | cell cycle | root apical meristem

ABSTRACT

Plant growth and development rely on a delicate balance between cell proliferation and cell differentiation. The root apical meristem (RAM) of *Arabidopsis thaliana* is an excellent model to study the cell cycle due to the coordinated relationship between nucleus shape and cell size at each stage, allowing for precise estimation of the cell cycle duration. In this study, we present a method for high-resolution visualization of RAM cells. This is the first protocol that allows for simultaneous high-resolution imaging of cellular and nuclear stains, being compatible with DNA replication markers such as EdU, including fluorescent proteins (H2B::YFP), SYTOX DNA stains, and the cell wall stain SR2200. This protocol includes a clarification procedure that enables the acquisition of high-resolution 3D images, suitable for detailed subsequent analysis.

1 | Introduction

Arabidopsis thaliana (from now on *Arabidopsis*) primary root is composed of various cell types arranged in concentric circles around the vascular bundle. All root cells originate from the stem cell niche (SCN), a region characterized by a low division rate. As cells move away from the SCN, they enter the meristem, where the proliferation rate is the highest in the root. Subsequently, they transit into the elongation zone, where cell division ceases, and cells attain their final size at the differentiation zone (Romero-Arias et al. 2017).

The cell cycle is a critical process that allows the duplication and equal distribution of the genetic material of a mother cell into two daughter cells, essential for growth and development in all living organisms. In eukaryotes, the cell cycle consists of four phases: Gap 1 (G1), DNA synthesis (S), Gap 2 (G2) and Mitosis (M) phases, along with a theoretical quiescent phase Gap 0 (G0). During the S phase, DNA synthesis occurs (Alberts et al. 2017; Velappan et al. 2017) and DNA replication initiates in the G1 phase, where regulatory pre-replication complexes associate with the DNA (Sclafani and Holzen 2007). Conversely, in the absence of growth-promoting conditions, cells enter the

This is an open access article under the terms of the [Creative Commons Attribution-NonCommercial-NoDerivs](https://creativecommons.org/licenses/by-nc-nd/4.0/) License, which permits use and distribution in any medium, provided the original work is properly cited, the use is non-commercial and no modifications or adaptations are made.

© 2025 The Author(s). *Plant Direct* published by American Society of Plant Biologists and the Society for Experimental Biology and John Wiley & Sons Ltd.

G0, restricting growth until conditions turn favorable (Velappan et al. 2017).

Labeling DNA with 5-ethynyl-2'-deoxyuridine (EdU), a thymidine analog, is a fast and robust assay widely used to detect DNA replication during the S-phase in plant cells. EdU is incorporated into newly synthesized DNA, allowing for precise detection (Buck et al. 2008; Kotogány et al. 2010; Nakayama et al. 2015). The EdU method has been used to determine the length of the cell cycle in the root apical meristem (RAM) of several plant species including *A. thaliana* (Hayashi et al. 2013; Pasternak et al. 2022), *Nicotiana tabacum* (Pasternak et al. 2017) and the fern *Ceratopteris richardii* (Aragón-Raygoza et al. 2020).

Previous studies indicate that the cell cycle length in the Arabidopsis meristematic zone is approximately 17.1 h, while in the elongation zone it extends to 30 h. The S-phase duration is 2.9 h in the meristematic zone and 8 h in the elongation zone (Hayashi et al. 2013; Savina et al. 2020; Pasternak, Kircher, and Palme 2021; Pasternak and Pérez-Pérez 2021). In contrast, Yin et al. (2014) suggest that the cell cycle length in root epidermal cells is around 14 h, with 6 h from M (anaphase) to G1, 8 h from S to G2, and 3 h from late G2 to M (metaphase). This estimate aligns with S-phase duration of 2 to 3 h observed in cell culture (Yin et al. 2014; Pasternak et al. 2022). Additionally, recent data suggest that the G1 stage length varies from approximately 2 h near the elongation zone to over 20 h in stem cells and newly emerging cells from the SCN (Echevarria et al. 2022).

In eukaryotic cells, including plants, the shape and size of the nucleus vary significantly during the cell cycle transitions, providing an estimate of the cell cycle length (Alberts et al. 2017; Chu et al. 2017; Efremov et al. 2022). Significant differences in the nuclei sizes are observed between different tissue layers, such as trichoblast (T) and atrichoblast (AT) cells, particularly at the G1–G0 transition. Similar variations are also observed along the longitudinal axis (Pasternak et al. 2022), highlighting the spatial variation in nuclear sizes within the root structure.

Throughout the cell cycle, nuclei can be visualized using chromatin labeling with DNA stains or through fluorescent protein fusion to nuclear proteins (Goto et al. 2021). Common nuclear stains used in fixed cells include DAPI (4,6-diamidino-2-phenylindole) and Hoechst (Mathur et al. 2012; Chowdhury et al. 2022). Both DAPI and Hoechst are blue-fluorescent stains that strongly bind to adenine–thymine-rich regions in the minor groove of double-stranded (ds) DNA (Bucevičius et al. 2018; Karg and Golic 2018). Other ds DNA-binding labels are the SYTOX dyes (Hayashi et al. 2013), which are available in different fluorescent color variants (blue, green, orange, and deep red), making them a versatile tool for fluorescence microscopy, flow cytometry, and microplate applications (Truernit and Haseloff 2008; Grootjans et al. 2016).

In the case of Arabidopsis, various nuclear reporter genes have been used for in vivo imaging using confocal laser scanning microscopy (CLSM). An example is the HISTONE 2B::YELLOW FLUORESCENT PROTEIN fusion (H2B::YFP) (Chytilova et al. 2000; Boissard-Lorig et al. 2001), allowing for detailed visualization of nuclear dynamics during cell cycle progression in vivo.

Nuclear reporters can be used in combination with dyes that label the plant cell wall (like propidium iodide, PI) or inner membrane organelles such as Golgi apparatus and the vacuolar membrane (like FM4-64) (Musielak et al. 2015; Helariutta et al. 2000). The application of these dyes result in a strong labeling of the epidermis and cortex/endodermis that can mask the signal from the stele, which can be much weaker, hindering the acquisition of images from inner layers of the root due to signal saturation (Musielak et al. 2015; Musielak et al. 2016). Additionally, it is not uncommon for the emission of these dyes in the red spectrum to interfere with that of red fluorescent proteins (RFP), which are traditionally used to highlight nuclei in cell cycle studies (Musielak et al. 2015).

An appropriate alternative to these compounds are the blue-range emitting dyes like SCRI Renaissance 2200 (SR2200) or calcofluor white (CFW) that bind to the plant cell wall with high affinity and specificity (Kurihara et al. 2015; Musielak et al. 2015; Musielak et al. 2016; Imoto et al. 2021). However, the emission of these dyes interferes with emission ranges of traditional nuclear stains like DAPI or Hoechst, which hinder double stains of nuclear and cell membrane in plants.

Most of the cell cycle studies have been conducted in the meristem of developing roots using 2D images, although there are some cases when 3D imaging has been employed (Lavrekha et al. 2017). 3D imaging enables to capture the high complexity of cell cycle dynamics occurring along the root meristem, offering a more precise and comprehensive depiction of cellular processes taking place in both the longitudinal and radial axes of the developing primary root.

In various studies, 3D maps of the RAM were generated using roots that were double-labeled for cell membrane/wall and nuclei (Schmidt et al. 2014; Lavrekha et al. 2017; Pasternak et al. 2017; Pasternak, Kircher, and Palme 2021; Pasternak and Pérez-Pérez 2021; Pasternak et al. 2022), and EdU and nuclear dyes (Hayashi et al. 2013; Pasternak and Pérez-Pérez 2021; Pasternak et al. 2017; Pasternak et al. 2022). However, it has not yet been developed a method that offers the possibility to visualize in 3D the cell DNA labeled with EdU, nuclear dyes, and the stained cell wall. This approach could facilitate the analysis of cell volumes, volumes and shapes of the nuclei, and DNA replication across various domains of the RAM (Pasternak and Pérez-Pérez 2021).

Here, we present a new protocol that allows imaging of triple-labeled RAM, using EdU with several fluorescent cellular stains and nuclear gene reporters optimized to construct a 3D map. By combining imaging with bioinformatic tools, this protocol allows a precise analysis of the cell cycle dynamics within the RAM.

2 | Results

2.1 | Detection of DNA Replication in the RAM of Primary Roots With SR2200 and Nuclear Markers

EdU incorporation has been widely used for the analysis of the cell cycle and DNA replication in the Arabidopsis RAM. However, its combination with different cell wall and nuclear

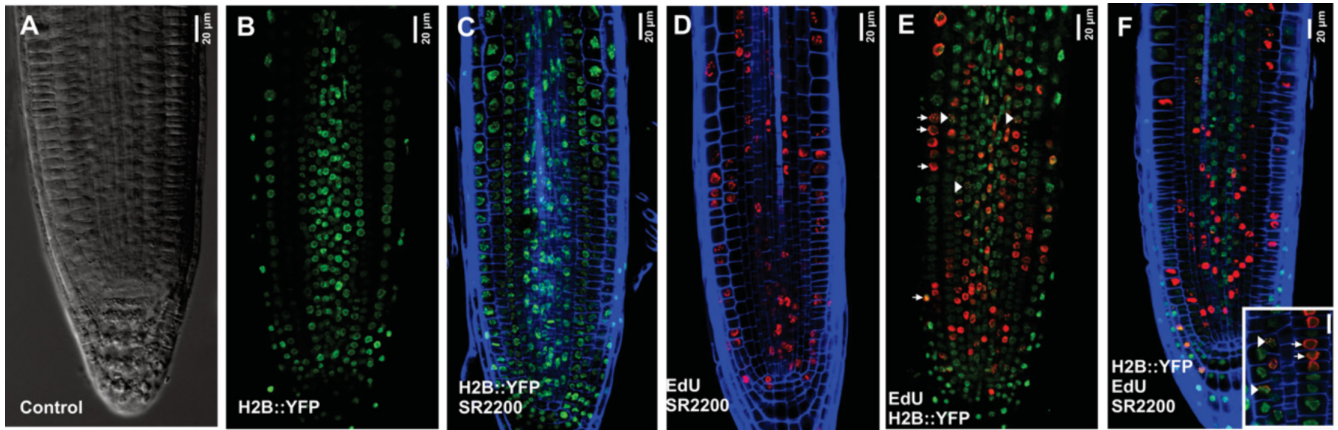


FIGURE 1 | Single confocal plane images of longitudinal sections of the *Arabidopsis* roots fixed and stained. (A) Widefield image. (B) H2B::YFP line fixed with FA and permeabilized displaying the YFP signal (green). (C) Confocal image of an H2B::YFP root stained with SR2200. (D) Confocal image of EdU- Eterneon-labeled cells and SR2200-stained cells from the meristem region of 1 h EdU-treated root tips. (E) EdU/H2B::YFP line labeled root tips. EdU-Eterneon-labeled cells is red color specifically labels nuclei undergoing DNA Replication, while H2B::YFP-green labels all nuclei. (F) Confocal image of EdU/H2B::YFP line labeled root tips and cell wall staining with SR2200. Insets show EdU-Eterneon-labeled cells distributions in whole and speckled patterns and cell wall staining. The white arrowhead marks speckled pattern, while white the arrow marks the whole pattern of nuclei in the DNA replication. The roots were not cleared, and to ensure proper dye incorporation, they were subjected to fixation and vacuum infiltration. Scale bars: 20 μ m (A–F), 10 μ m (F insets).

labeling, excluding propidium iodide (PI), has not been reported. To obtain a detailed 3D map of DNA replication cell events along the stem cell niche and in the meristematic zone of the RAM, we first analyzed the potential effects of fixation on YFP fluorescence from H2B::YFP plants (Figure 1A,B).

Plants were fixed with 4% formaldehyde in PBS buffer (pH 7.0) and vacuum infiltration. The samples were vacuum infiltrated (80 KPa) for 1 h (Data S2 and S3). We did not observe autofluorescence in control wild-type plants (Figure 1A) that were fixed and vacuum infiltrated. Additionally, we did not observe a decrease in YFP fluorescence after fixation and vacuum infiltration (Figure 1B). Then, we used different concentrations of SR2200 (cell wall marker) and nuclear stains to obtain a uniformly stained sample of longitudinal primary root sections (Data S4). At a concentration of 1% SR2200, all cell walls were clearly labeled along the longitudinal axis, and the quiescent center (QC) could be observed (Figures 1C,D).

Next, we combined EdU staining with SR2200 (Figure 1D) or nuclear labeling with H2B::YFP (Figure 1E,F). The EdU-Eterneon-labeled nuclei were observable along the RAM (Figure 1D–F) in both whole and speckled patterns. It is interesting that the whole pattern has been associated with early DNA replication, while the speckled pattern is linked to heterochromatic regions during late DNA replication (Kotogány et al. 2010; Hayashi et al. 2013).

In roots of H2B::YFP plants treated with EdU, the whole pattern is characterized by the EdU signal overlapping with the nuclear signal of H2B::YFP, whereas the speckled pattern is characterized by patches of EdU signals distributed throughout the nuclear signal of H2B::YFP (Figures 1E–F and S1A).

We then attempted the triple labeling with EdU, SR2200, and H2B::YFP in the corresponding transgenic plant line.

In H2B::YFP and EdU-treated roots, we observed the typical whole and speckled patterns of the EdU dye, while SR2200 strongly stained cell walls at stele layers of the RAM (Figures 1F and S1A). In a separate set of experiments, we conducted a similar analysis using calcofluor white (CFW) instead of the SR2200 to label the cell wall (Figure S1B). Although we did not observe changes in the labeling of the cell wall of the stele layers, the obtained signal was weaker compared to that of samples stained with SR2200 (compare Figure S1B with S1C).

SR2200 is a blue-fluorescent dye whose emission range overlaps with the nuclear stains DAPI and Hoechst. Therefore, as a nuclear stain we used SYTOX Green which has an emission peak at 523 nm (green) when excited at 488 nm light (Hayashi et al. 2013; Grootjans et al. 2016). However, although SYTOX Green exhibits a strong preference for double-stranded DNA (dsDNA), it can also bind to RNA. To reduce the background fluorescence resulting from the dye binding to cytosolic RNA, we included an RNase treatment step before SYTOX Green labeling (Figure S1D and Data S2 and S3). As a result, all roots stained with SYTOX Green showed a clear and uniform nuclear signal and low fluorescence in the cytoplasm (Figure 2A), similar to the pattern observed in roots stained with Hoechst (Figure 2B,C).

We additionally tested SYTOX Orange dye, that emits in the red spectral range. Like SYTOX Green, SYTOX Orange fluorescence was limited to the nuclei and only low fluorescence was observed in the cytoplasm (Figures 2D and S2A–D). Mitotic figures were clearly distinguished when using either SYTOX Green or SYTOX Orange, which can be useful to identify the progression of cell division (Figure 2A,D). When roots were stained with SYTOX Green and EdU, the signals of both overlapped (Figure 2E), making this combination useful to identify cell-cycle stages and mitotic figures.

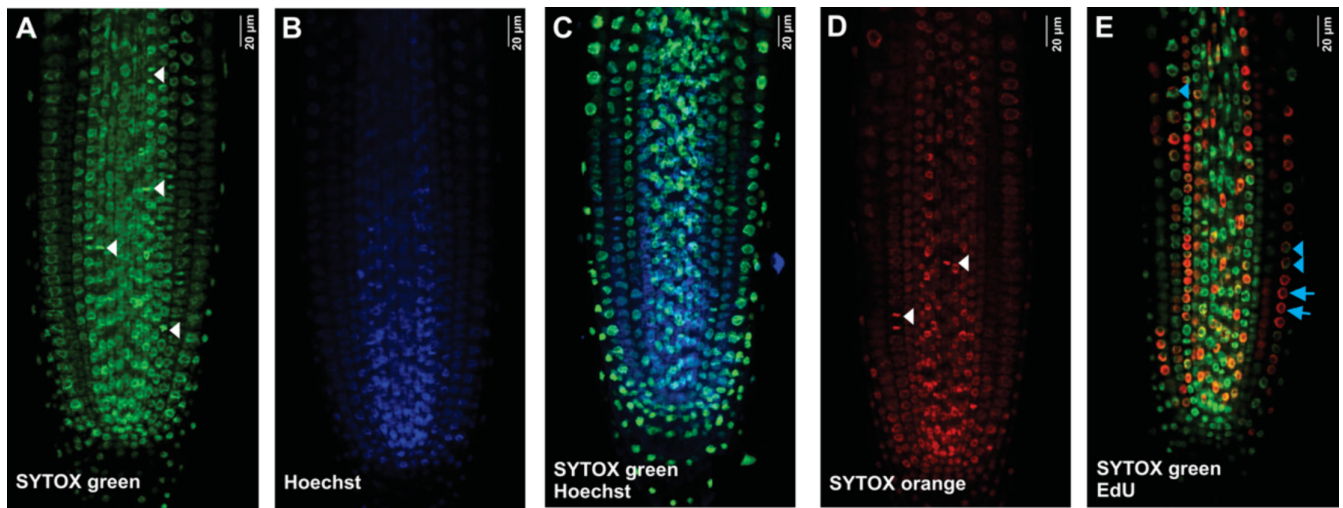


FIGURE 2 | Single confocal plane images of Arabidopsis roots staining and EdU-Eterneon click reaction, without clearing protocol. (A) Confocal image of Col-0 root treated and stained with SYTOX green. SYTOX Green stain binds nucleic acids of the nucleus. (B) Col-0 root treated and stained with Hoechst 34580. (C) Confocal image of double dye Hoechst 34580/SYTOX Green from Col-0 root. The SYTOX Green and Hoechst 34580 showed a clear nuclei signal. (D) Confocal image of Col-0 root treated and stained with SYTOX Orange. (E) EdU/SYTOX Green labeled root tips. EdU-Eterneon are red color marks nuclei undergoing the DNA replication, while SYTOX Green marks nuclear acids. White arrowhead marks mitotic figures. The blue arrowhead marks a speckled pattern, while the blue arrow marks the whole pattern of nuclei in the DNA replication. Scale bars = 20 μm (A–E).

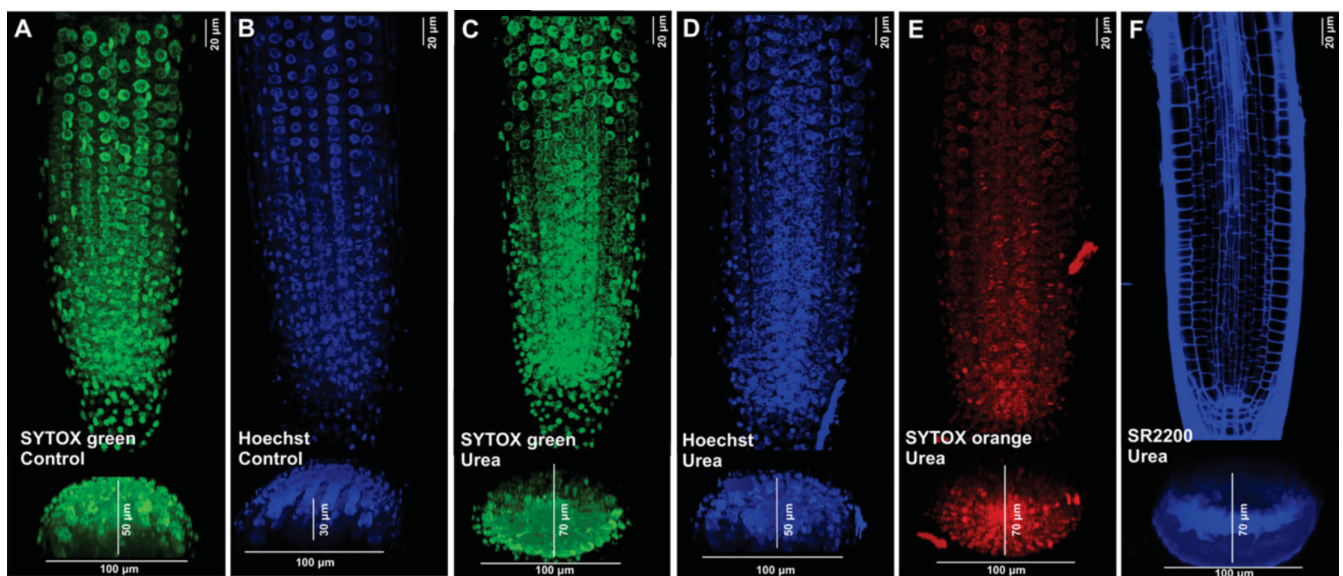


FIGURE 3 | 3D reconstruction of roots cleared following the scale-based method and stained with nuclear and cell wall dyes. (A, B) Maximum intensity projection of a z-stack of SYTOX-stained (A), or Hoechst 34580-stained (B) Arabidopsis roots without clearing. (C–F) Scale-based method in SYTOX-stained (C, E), Hoechst 34580 (D), and SR2200 (F). Scale bars = 20 μm .

2.2 | 3D Reconstruction of DNA Replication in the Primary Root RAM With Cellular Resolution

To create a 3D map of nuclei in the S-phase of the primary root tip, we acquired z-stack images of the RAM labeled either with SYTOX Green or Hoechst (control) nuclear dyes (Figure 3A,B). However, detecting the fluorescence from cells located far away from the coverslip surface was challenging and often quite weak and diffuse, particularly in deeper layers of the stele, due to the thickness and opacity of the root. Therefore, we applied the scale-based method (Warner et al. 2014) to clarify and adjust the refractive index of roots stained independently with SYTOX Green, SYTOX Orange, or Hoechst (Figure 3C–E).

To accomplish this, Arabidopsis roots were first incubated with the staining solution for 72 h (Data S2 and S3), followed by treatment with the scale-based method (Data S2 and S3) for 3 days to 1 week, depending on the root thickness. The scale-based method (Warner et al. 2014) preserved the fluorescence of SYTOX dyes, Hoechst, and SR2200 in the stele and deeper tissues of the RAM (Figure 3C–G), demonstrating its effectiveness for 3D image acquisition in the RAM. The fluorescence of SYTOX, Hoechst, or SR2200 was clearly observed even after storing the roots in the scale-based solution for 4 days (Figure 3C–G).

We analyzed the 3D projection of primary roots with different nuclear dyes treated with or without the scale-based method

(Figure 3). The fluorescence of SYTOX in roots without the scale-based method was detectable to approximately 50 μm depth from the epidermis layer (Figure 3A). In contrast, the signal from nuclei in roots treated with the scale-based method could be obtained at depths greater than 70 μm from the epidermis layer (Figure 3C,E).

A similar result was observed with Hoechst staining (compare Figure 3B with 3D). The scale-based method also allowed to enhance the signal of nuclear markers in the vascular bundles for 3D reconstruction (Figure 3C–E).

An alternative clearing solution, ClearSee, was developed as an optical clearing method for plant tissues that preserves the emission of fluorescent proteins (Kurihara et al. 2015; Imoto et al. 2021). Therefore, we tested the compatibility of the ClearSee method with SYTOX staining (Figure S2E). Although the ClearSee method allowed us to observe cell walls labeled with either the SR2200 or CFW dyes, and nuclei stained with either Hoechst, EdU, or H2B::YFP in 3D reconstructions, it appeared to be incompatible with SYTOX staining. The signal from SYTOX was eventually lost from the nuclei, making it impossible to generate a 3D reconstruction (Figure S2E).

We then analyzed the compatibility of the H2B::YFP line treated with EdU (Figure 4A–C) and roots treated with SYTOX Green staining and EdU-Eterneon using the scale-based clearing method (Figure 4D–F). Both H2B::YFP and SYTOX Green exhibited distinct nuclear signals and low fluorescence in the cytoplasm. Meanwhile, the EdU-Eterneon signals displayed the characteristic speckled and whole patterns observed in previous experiments (Figure 4). Afterwards, we performed 3D complete RAM imaging. H2B::YFP, SYTOX Green, and EdU, alone or in combination, showed defined nuclear signals along 70 μm of the thickness of the primary root tissues (Figure 4). Furthermore, we demonstrated how this technique allows the detection of

nuclei in the RAM using the scale-based method; the whole root of SR2200/H2B::YFP (Movie S1) and EdU-SYTOX Green staining (Movie S2). The fluorescence signals of nuclei were clearly observed in the epidermis and internal regions of the root (Movies S1 and S2). Moreover, we obtained z-stack images at high resolution using EdU, showing nuclei undergoing DNA replication in the epidermis and vascular bundles (Movie S3). These results suggest that our method preserves specific H2B::YFP expression, as well as SYTOX or EdU stains, in a 3D reconstruction of the primary root.

2.3 | Three Color 3D Reconstructions of the Primary RAM With Cellular Resolution

To generate a 3D reconstruction of the entire RAM displaying the three labels of interest, we analyzed H2B::YFP roots treated with EdU-Eterneon and SR2200 (Figure 5), as well as wild-type roots stained with SYTOX Green, SR2200, and treated with EdU-Eterneon (Figures 6 and S2F). In both cases, SR2200 staining was observed in the cell walls of epidermal cells and the stele throughout the entire RAM (Figures 5A and 6A). Meanwhile, H2B::YFP/SYTOX Green and EdU-Eterneon-labeled cells were distinctly visible in the nuclei, showing their characteristic distribution patterns (Figures 5B,C and 6B,C).

For EdU-Eterneon signal, the whole and speckled patterns were still there (Figures 5E and 6E). The whole pattern distribution of the EdU-Eterneon signal throughout the nucleoplasm, overlapped with the nuclear signal of H2B::YFP (Figure 5E) and SYTOX Green (Figure 6E), whereas the speckled pattern could be observed both in the EdU and H2B::YFP/SYTOX Green channels throughout the nucleoplasm (Figures 5E and 6E). In addition, we observed that the cell walls (stained with SR2200) in both epidermal cells and internal tissues were stained across the observable depth which was around 70 μm (Figures 5A,E

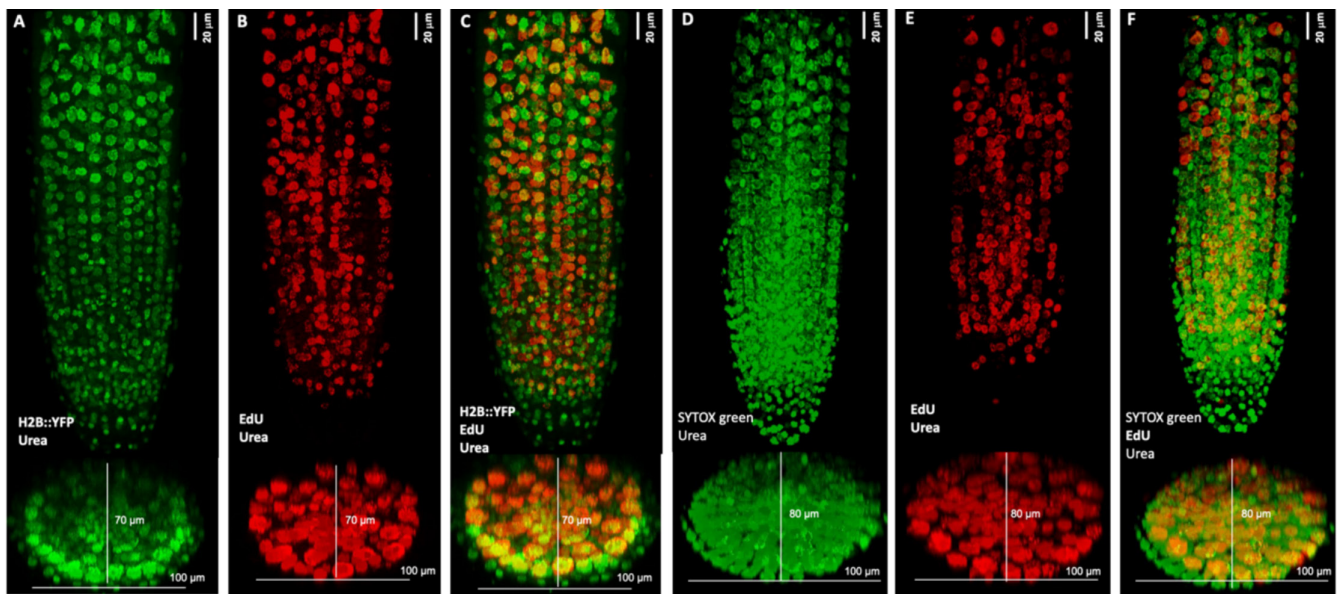


FIGURE 4 | 3D reconstruction of Arabidopsis roots treated with a scale-based method and pre-stained. (A–C) 3D reconstruction of 70 serial optical sections of H2B::YFP and EdU-Eterneon-labeled cells in roots using a scale-based method. EdU-Eterneon labeling (red) marks nuclei undergoing DNA replication, while H2B::YFP (green) labels the entire nucleus. (D–F) 3D projection of roots SYTOX-stained and EdU. EdU-positive nuclei (red) marks nucleus with DNA replication and SYTOX Green (Green) marks nuclear acids. Scale bars = 20 μm .

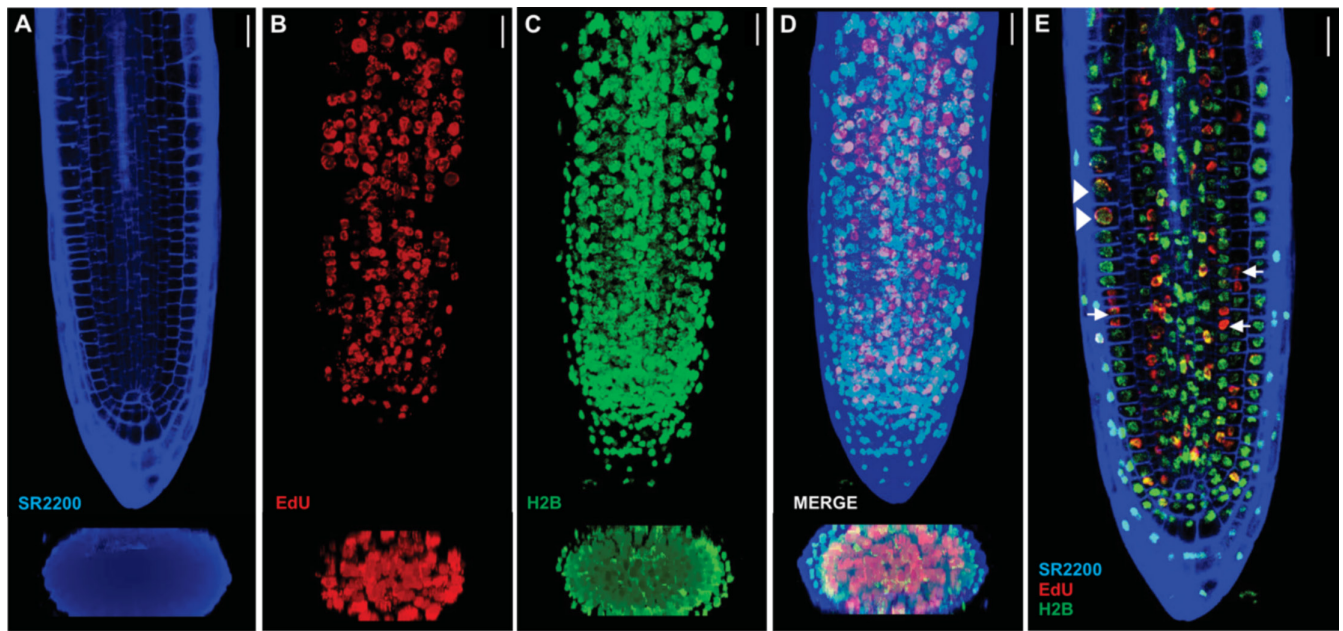


FIGURE 5 | Confocal microscopic images of a scale-based method root with H2B::YFP, EdU-Eterneon and SR2200. 3D reconstruction of 70 serial optical sections obtained from the same root as in (A) SR2200, (B) EdU-Eterneon-labeled cells, and (C) H2B::YFP views. The signals of H2B::YFP, EdU, and SR2200 are represented in green, red, and blue, respectively. (D) Merge and (E) single confocal plane image of a root staining with EdU-H2B::YFP-SR2200. The white arrowhead marks a speckled pattern, while the white arrow marks the whole pattern of nuclei in DNA replication. Scale bars = 20 μ m.

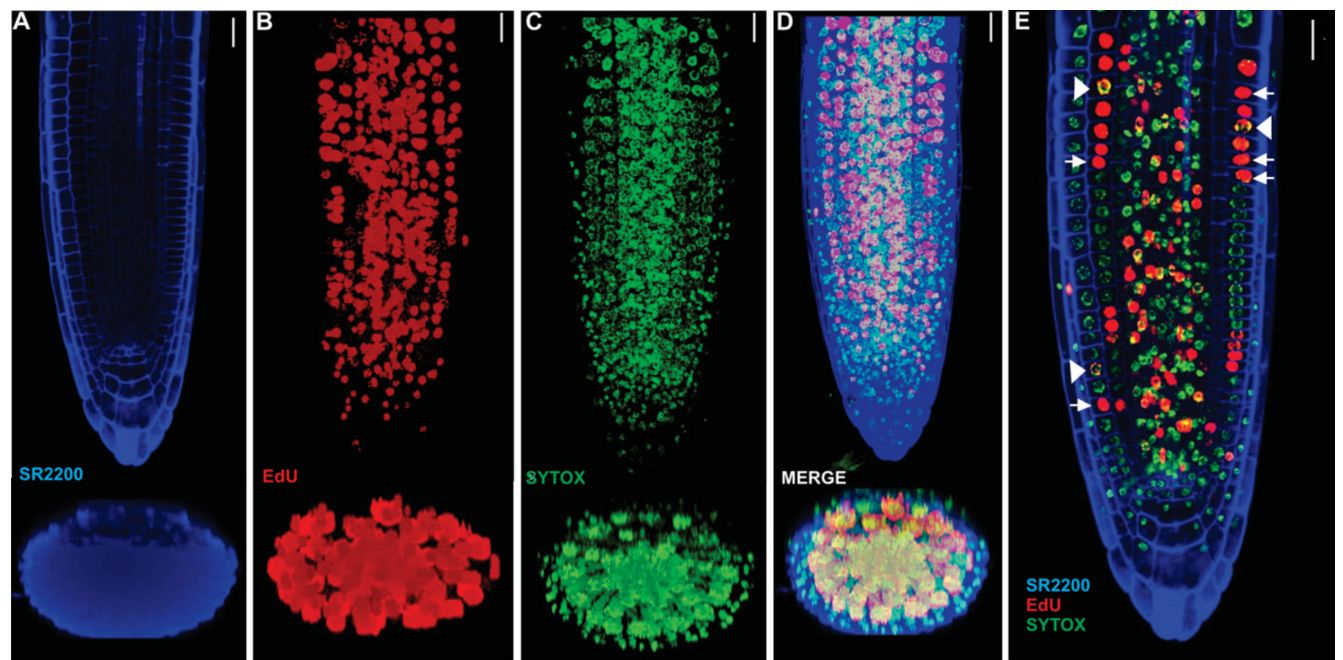


FIGURE 6 | Application of the scale-based method for the visualization of DNA replication in Arabidopsis root and stained with chemical dyes. 3D reconstruction of 70 serial optical sections obtained from the same root as in (A) Single plane and 3D reconstruction of SR2200, (B) EdU-Eterneon-labeled cells, (C) SYTOX-stained, (D) merge, and (E) single confocal plane image of a root stained with EdU-SYTOX-SR2200. An arrowhead and an arrow indicate a speckled nuclear pattern and a whole nuclear pattern, respectively. Scale bars = 20 μ m.

and 6A,E and Figure S2F). Movies S4 and S5 support the suitability of this protocol to visualize the whole RAMs harboring the H2B::YFP, EdU and SR2200 labels in a 3D reconstruction (Movies S4 and S5).

With these data, we demonstrated that the combination of EdU-H2B::YFP-SR2200 and EdU-SYTOX Green-SR2200 (Figures 5 and 6) can be used to visualize DNA replication, nucleoplasm, and cell wall at high resolution.

2.4 | Cell and Nuclei Segmentation With Deep Learning

Cell segmentation plays a key role in biological image analysis, which relies on high-quality images for the accurate identification of individual cells. Therefore, we standardized the images and automated the segmentation based on nuclear and cell wall markers of the H2B::YFP-EdU-SR2200 and SYTOX Green-EdU-SR2200 triple stains (Figure 7). The proposed pipeline uses a deep learning approach to automatically segment the nuclei and the cells. For nuclei segmentation in 3D images, we employed cellpose (Stringer et al. 2021; Eschweiler et al. 2022), a deep learning model trained on a diverse range of images of nuclei that enables the generalization to different types of nuclei images (Figure 7A,D).

For the automatic segmentation of RAM cells from 3D confocal images, we used DRPP methods (Pasternak, Falk, and Paponov 2021; Schmidt et al. 2014) and Plant-Seg (Wolny et al. 2020). However, our data show better segmentation performance with Plant-Seg (Figure 7C,F).

For both the EdU-H2B and EdU-SYTOX, the nuclear signals were of high quality, allowing the cellpose deep-learning model to segment accurately each nucleus, despite the large number of nuclei observed (Figure 7A,B,D,E). Cell segmentation using Plant-Seg was conducted using the SR2200 cell wall signal (Figure 7C,F).

Altogether, the proposed approach used to visualize nuclei and cell walls can be combined with deep learning algorithms to automatically identify and segment the nuclei and cell wall, even in densely packed cells characteristic of the root meristem into 3D images. This methodology holds the potential for counting nuclei, to calculate cell volume, to perform cell wall area measurements, and to extract other geometric features of the cells (Montenegro-Johnson et al. 2019).

The Cellpose algorithm generates a unique identifier for each segmented nucleus, enabling precise identification of the region each nucleus occupies. This allows for the calculation of various metrics, such as volume, roundness, surface area, lengths along the x, y, and z axes, centroid position, and more. It is important to note that Cellpose segmentation uses voxel coordinates, which must be converted to real-world coordinates using the voxel size in micrometers. This figure shows the distribution of nuclei volumes for the image (Figure 8A). We also analyzed the 3D segmented nuclei to extract several of their morphological features. The scatter plot on a logarithmic scale (Figure 8B) reveals a clear linear relationship between the volume and surface area of the nuclei. The data indicate that nuclei are smaller near the stem cell niche and increase in size as we move away from it.

3 | Discussion

The aim of this study was to develop an efficient and robust method that allows for simultaneous imaging of both cell and nuclear stain channels, along with DNA replication, to create a detailed 3D map of cellular structures within the RAM. This

method is compatible with EdU labeling and various nuclear stains, such as SYTOX or DAPI, as well as nuclear reporters utilizing fluorescent markers. Additionally, cell outlines were stained using the cell wall stain SR2200, making this approach a valuable tool for 3D volumetric cell extraction. The combination of these triple stains enables the generation of detailed 3D maps with cellular resolution.

To our knowledge, no existing triple-stain methods currently allow for the simultaneous visualization of nuclei number, DNA replication, and cell walls using different fluorophores, while also enabling accurate and widely applicable 3D segmentation for digital reconstruction along the RAM (Pasternak et al. 2015; Pasternak and Pérez-Pérez 2021). For example, recently Vijayan et al. (2024), presented a new set of computational tools that allows the segmentation of double stains with TO-PRO-3-stained nuclei and SR2200-stained cell. However, the TO-PRO-3 staining was variable and often quite weak and diffuse, particularly in deeper layers (Vijayan et al. 2024), this issue did not occur with SYTOX in our protocol. Furthermore, several quantitative methods available for 3D analysis only study cell cycle and nuclear organization independently of cell volume or they analyze nuclear organization and cell volume separately (Pasternak et al. 2017; Pasternak and Pérez-Pérez 2021; Pasternak, Kircher, and Palme 2021; Pasternak et al. 2022). However, our method allows for high-quality simultaneous imaging of both cell, nuclei, and DNA replication.

To address this gap, we proposed a novel approach for visualizing DNA replication events by applying 3D cell segmentation to triple-labeled samples stained with SR2200-SYTOX Green-EdU or SR2200-H2B::YFP-EdU, and cleared using the scale-based method (Warner et al. 2014). This strategy enables us to obtain samples uniformly stained along the entire root structure, facilitating the acquisition of optical sections with high contrast on a confocal microscope of cell, nuclei, and the DNA replication. Interestingly, although EdU incorporation has been widely used to determine and analyze DNA replication (Buck et al. 2008; Kotogány et al. 2010; Hayashi et al. 2013; Nakayama et al. 2015), recent studies have shown that the duration of EdU incubation influences the detected cell cycle stages. Short EdU incubation (20–30 min) specifically marks cells actively replicating DNA, while longer incubation allows the identification of both S and G2 phases. Additionally, very long incubation (16–24 h) enables the detection of EdU-negative cells with extended G1 phases (Pasternak and Pérez-Pérez 2021). Therefore, our method can be adapted to different incubation times to analyze various cell cycle stages and DNA replication dynamics more precisely.

In most studies, cell cycle events are typically analyzed using single 2D images (Goldy et al. 2021; Lasok et al. 2023). The advantage of this approach lies in its simplicity, as sample staining is easier and extensive permeabilization and clearing protocols are not required. However, for a deeper understanding of cell cycle progression and DNA replication, a quantitative 3D analysis of cell size, nuclei shape, and cell cycle phase is necessary. Therefore, there is a need for a method that can provide a more accurate and comprehensive depiction of cellular processes and cell cycle progression throughout the root structure.

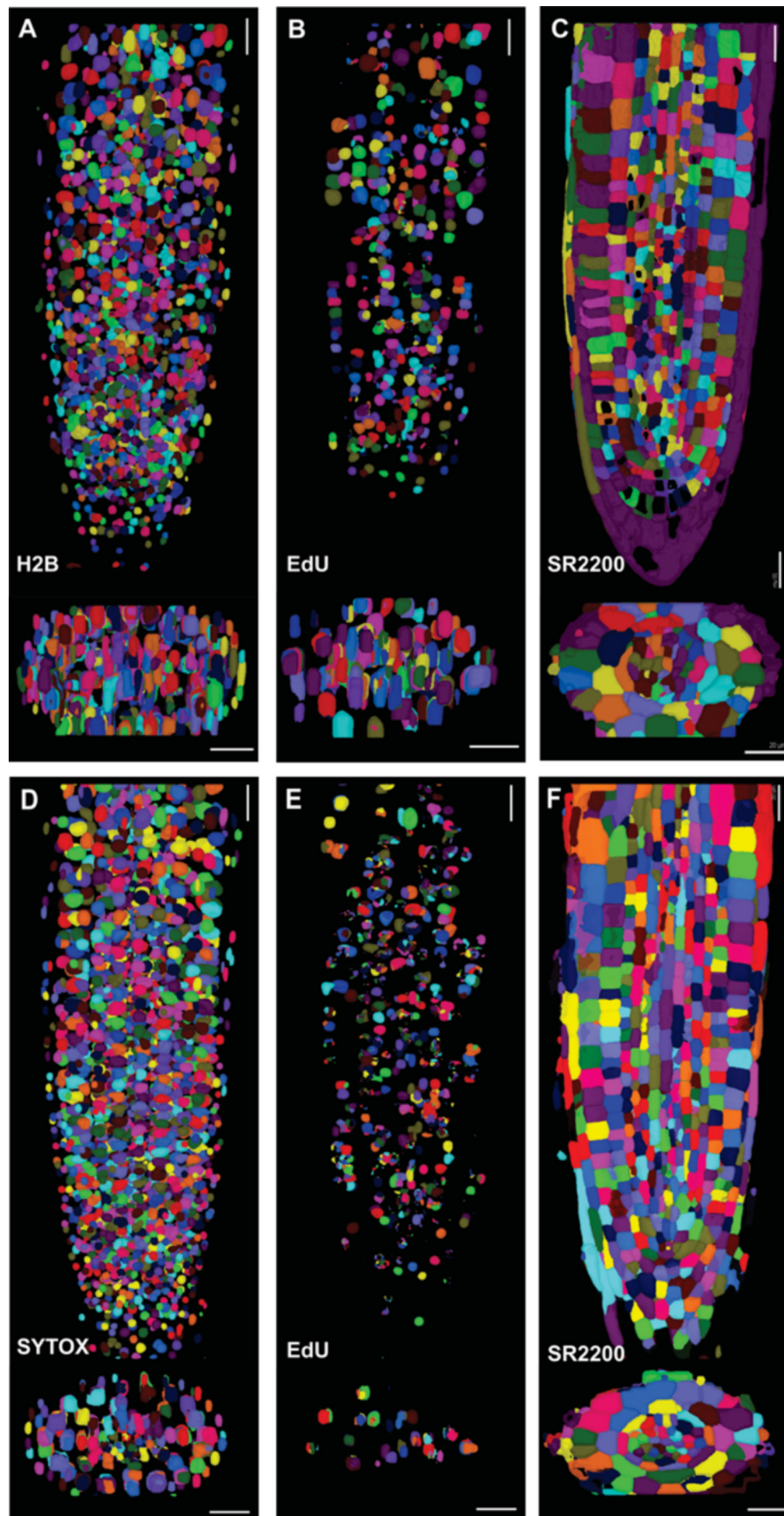


FIGURE 7 | 3D visualization of segmented cells, nucleus and DNA replication. Segmentation reconstruction from the same root. (A) 3D segmentation of nucleus (H2B::YFP) and (D) nucleus stained by SYTOX. (B, E) 3D segmentation of cells in phase S (EdU staining of DNA replication). (C, F) 3D image of cell wall stained by SR2200. Scale bars = upper and lower 20 μm (A–F).

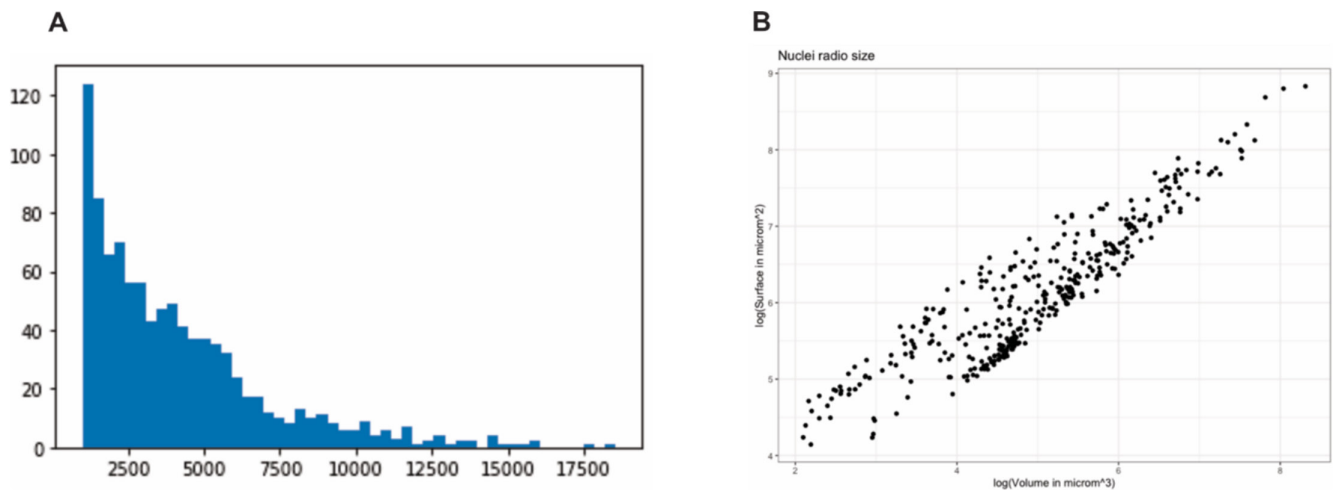


FIGURE 8 | Applications of nuclei segmentation. (A) Distribution of nuclei volume in the roots of *Arabidopsis thaliana*. (B) Scatter plot showing the relationship between nuclei volume and surface area on a logarithmic scale.

Several studies in *Arabidopsis* have proposed methods for cell segmentation from 3D root samples. The more commonly used approaches typically employ independent imaging of nuclei or cell walls (Liu et al. 2013; Wolny et al. 2020; Kerstens et al. 2020; Fridman et al. 2021; Pasternak and Pérez-Pérez 2021). These methods, such as MorphoGraphX, focus on enhancing images of nuclei and cell membranes, followed by the detection of nuclei or intermembranous regions to identify individual cells (Fridman et al. 2021; Strauss et al. 2022; Vijayan et al. 2024). However, only a limited number of studies in *Arabidopsis* have utilized simultaneous imaging of both cell walls and nuclei to guide a mixed 3D segmentation. (Schmidt et al. 2014; Lavrekha et al. 2017; Pasternak et al. 2017; Pasternak and Pérez-Pérez 2021; Vijayan et al. 2024). Our method enables simultaneous imaging of cells, nuclei, and DNA replication with high resolution, allowing for independent 3D segmentation of each component. Additionally, a mixed 3D model could be developed by integrating data from nuclei, cell walls, and DNA replication and by incorporating a neural network similar to those used in studies of 3D segmentation of myocardial cells (Sarkar et al. 2022).

While a single low-resolution 3D digital map of the RAM has previously been proposed using triple labeling of EdU, nuclei, and cell walls (Truernit and Haseloff 2008; Pasternak and Pérez-Pérez 2021), this method relied on propidium iodide for labeling the nuclei, which interferes with the signal of other markers in the red spectrum. Moreover, without proper treatment (time of de-ketonization is a crucial parameter), both nuclei and cell walls can be labeled simultaneously, resulting in suboptimal staining for 3D segmentation. In contrast, our staining method is compatible with red-emitting fluorophores, which are widely used as markers for cell cycle phases (Yin et al. 2014; Desvoyes et al. 2020; Echevarría et al. 2021; Echevarría et al. 2022). Additionally, unlike propidium iodide, SR2200 specifically labels the cell wall and does not stain nuclei, making it ideal for high-resolution 3D imaging.

Interestingly, recent findings have shown that the RAM exhibits a positional gradient of G1 length along the longitudinal axis (Echevarría et al. 2022), although a similar cell cycle pattern

along the radial axis has not been described yet. Our staining method enables us to obtain high-resolution z-stacks necessary for constructing high-quality 3D models. This opens up possibilities for applications such as the detection of DNA replication and the analysis of cell cycle phase marker lines to study cell cycle length along the radial axis. Furthermore, the integration of the H2B::YFP line in our method could enable simultaneous imaging of other cellular or nuclear markers.

Finally, the method proposed in the present study has a wide range of potential applications, spanning from whole organs to subcellular analyses. Additionally, it could be adapted for use in other plant tissues, such as leaves, shoot apical meristem, or the gynoecium (Hayashi et al. 2013; Reyes-Olalde and de Folter 2019). Potentially, it could also be used with other cell wall (Ursache et al. 2018) and nuclear dyes (Boothe et al. 2017). Our method could also be applied in studies of the cell cycle length in plants using various cell cycle phase markers such as Cytrap (Yin et al. 2014) and PLaCCI (Desvoyes et al. 2020).

4 | Experimental Procedures

4.1 | Plant Material and Growth Conditions

Most of the *Arabidopsis* plants utilized in this study were in the Columbia-0 background, with the exception of the H2B::YFP reporter line (Boisnard-Lorig et al. 2001), that was engineered on the Landsberg erecta background. Three days old seedlings were grown on vertical plates with 0.2× Murashige Skoog (Murashige and Skoog 1962) salts (MP Biomedicals) supplemented with 1% sucrose (Tapia-López et al. 2008).

4.2 | Fixation Procedure

The detailed tissue fixation procedure is described in Data S2 and S3. Tissue fixation was performed with 4% formaldehyde diluted in 1× PBS at pH 7.0. Freshly prepared 4% formaldehyde solution was obtained from formaldehyde liquid solution (Sigma-Aldrich).

In our experience, formaldehyde and vacuum (−0.08 MPa) for 30 min work well for nuclear proteins and nuclear stains.

4.3 | EdU-Based Proliferation Assay

The detailed EdU assay procedure is described in Data S2–S4. The seedlings (3 days of germination) were placed in 0.5× liquid MS containing 10 μM EdU for 1 h to label cells undergoing S-phase. The plants were then fixed with 4% formaldehyde in PBS and EdU incorporation was detected with cocktail BaseClick (EdU Flow Cytometry Kit, Eterneon-Red 645 Azide, cat no: BCK647-IV-FC-S) for 30 min at room temperature (RT) in darkness. For one sample reaction, the following amounts of the kit components were mixed: 87.75 μL of PBS, 2 μL of catalytic solution (component F, kept frozen in small aliquots), 0.5 μL of Eterneon-Red 645 Azide (eterneon, component D), and 6.7 μL of additive buffer (component E, 100 mM CuSO₄). Many azide-labeled fluorochromes other than eterneon are available throughout the visible spectrum for multicolor labeling purposes. To prevent oxidation of the catalytic solution, the detection cocktail was prepared freshly. Although the BaseClick reaction is not light-sensitive, fluorochrome-containing solutions should not be exposed to strong light.

4.4 | Clearing Procedure

The detailed clearing and staining procedure are described in Data S2 and S3. Briefly, the plant material was transferred to the urea-clearing solution (scale-based method) and cleared under agitation at room temperature. For 2D root images clearing, an overnight/1 day clearing was sufficient. On the other hand, for 3D reconstructions, seedlings had to be kept in the clearing solution for at least 72 h. Applying vacuum for 20 min (−0.08 MPa) (one time per day) significantly improved the quality of clearing.

4.5 | Staining Procedure

The detailed clearing and staining procedure are described in Data S2–S4. For single Hoechst (Thermo Fisher Scientific), SYTOX (Thermo Fisher Scientific), calcofluor white (Sigma-Aldrich), or SR2200 (Renaissance Chemicals), stains were prepared directly in staining solution, and the seedlings were stained for 24 or 72 h, applying vacuum (−0.08 MPa) for 20 min every 24 h. Next, Basic Hoechst, SYTOX, Calcofluor White, and SR2200 solution were removed and washed three times with 1 mL of HEPES at 10 μM (pH 7), then HEPES solution was removed, and then urea clearing solution was added to the seedlings for 2 days under gentle shaking at room temperature. Longer washing times do not diminish the signal from staining and help to further remove the remaining background noise. For longer storage of stained samples, the plates were covered to avoid light exposure.

For double staining of Arabidopsis roots with scale-based method (Warner et al. 2014) compatible with SR2200 and SYTOX, the following steps were performed: (i) the seedlings were stained with 1% SR2200 in staining solution for 24 or 72 h (Data S2 and S3) and applied vacuum (−0.08 MPa) for 20 min every 24 h; (ii) removed and washed three times with 1 mL of HEPES at 10 μM and pH 7;

(iii) removed the HEPES solution, and then the urea clearing solution was added with 0.15 μM of SYTOX to seedlings and stained for 24 or 72 h storing them in the dark and refrigerated at 4°C; (iv) the seedlings were washed in urea clearing solution for 2 days under gentle shaking at room temperature.

4.6 | Confocal Laser Scanning Microscopy (CLSM)

Fluorescent digital images were captured using Nikon A1 or Nikon A1R+laser scanning confocal heads coupled to an Eclipse Ti-E inverted microscope (Nikon Corporation, Tokyo, Japan) equipped with a motorized stage (TI-S-E, Nikon) and controlled through NIS Elements C v.5.00 software. Images were acquired using a Plan Apo lambda 20× (N.A. 0.75) or Plan Apo VC 60× WI DIC N2 (N.A. 1.2) objective lens. Fluorochromes were excited either with 405 nm (Hoechst 34580, SR2200, calcofluor white), 488 nm (YFP, SYTOX Green), 546 nm (SYTOX Orange) or 633 nm (Eterneon-Red 645) laser lines in a sequential mode. The respective emissions were read in the 425–475 nm, 500–550 nm, 560–620 nm, and 700–740 nm wavelength ranges using the filter cubes provided by the manufacturer, with a pinhole aperture set at 12.77 mm. For 3D reconstructions, we started acquiring z-stacks with Plan Apo VC 60× WI at Nyquist resolution in Z, then we acquired z-stacks with Plan Apo lambda 20× with 0.7–1 μm of interval and then we realized volumetric projections of both z-stacks, and we did not find differences in 3D reconstructions; because the scanning time is significantly lower at 20× (diminishing photobleaching of our fluorescent stains), we chose to acquire the z-stacks just with the 20× objective.

Acknowledgments

We are most grateful to Dra. Diana Belen Sánchez-Rodríguez and Dr. Marco Tulio Solano de la Cruz for technical support. We thank the Dirección General de Asuntos del Personal Académico (DGAPA-UNAM) for a postdoctoral fellowship to JIRO. This work in the Álvarez-Builla laboratory was financed by the PAPIIT UNAM IN213524, IN203220, IN206220, IN203223, IN211721, and Conahcyt 102959 and CF-2023-G-708. This project has been made possible in part by grant number 2023-329644 from the Chan Zuckerberg Initiative DAF, an advised fund of the Silicon Valley Community Foundation.

Author Contributions

Conceptualization: J.I.R.O. and E.R.A.B. Methodology: J.I.R.O., M.T.R., V.P.K., G.C.J., and E.R.A.B. Validation: J.I.R.O., M.T.R., V.P.K., G.C.J., P.H.H., G.C., and A.J.A.G. Formal analysis: P.H.H., G.C., and A.J.A.G. Investigation: J.I.R.O., G.C.J., M.D.S., B.G.P., A.G.A., and E.R.A.B. Writing – original draft: J.I.R.O., M.D.S., B.G.P., A.G.A., and E.R.A.B. Writing – review and editing: J.I.R.O. and E.R.A.B. Visualization: J.I.R.O., G.C.J., P.H.H., A.G.A., and E.R.A.B. Supervision: M.D.S., B.G.P., A.G.A., and E.R.A.B. Project administration: E.R.A.B. Funding acquisition: M.D.S., A.G.A., G.C.J., and E.R.A.B.

Conflicts of Interest

The authors declare no conflicts of interest.

Peer Review

The peer review history for this article is available in the [Supporting Information](#) for this article.

References

- Alberts, B., A. Johnson, J. Lewis, et al. 2017. *Molecular Biology of the Cell*. 7th ed. New York: Garland Science.
- Aragón-Raygoza, A., A. Vasco, I. Blilou, L. Herrera-Estrella, and A. Cruz-Ramírez. 2020. "Development and Cell Cycle Activity of the Root Apical Meristem in the Fern *Ceratopteris richardii*." *Genes (Basel)* 11, no. 12: 1455. <https://doi.org/10.3390/genes11121455>.
- Boisnard-Lorig, C., A. Colon-Carmona, M. Bauch, et al. 2001. "Dynamic Analyses of the Expression of the Histone::YFP Fusion Protein in Arabidopsis Show That Syncytial Endosperm Is Divided in Mitotic Domains." *Plant Cell* 13, no. 3: 495–509. <https://doi.org/10.1105/tpc.13.3.495>.
- Boothe, T., L. Hilbert, M. Heide, et al. 2017. "A Tunable Refractive Index Matching Medium for Live Imaging Cells, Tissues and Model Organisms." *eLife* 6: e27240.
- Bucevičius, J., G. Lukinavičius, and R. Gerasimaitė. 2018. "The Use of Hoechst Dyes for DNA Staining and Beyond." *Chem* 6: 18.
- Buck, S. B., J. Bradford, K. R. Gee, B. J. Agnew, S. T. Clarke, and A. Salic. 2008. "Detection of S-Phase Cell Cycle Progression Using 5-Ethynyl-2'-Deoxyuridine Incorporation With Click Chemistry, an Alternative to Using 5-Bromo-2'-Deoxyuridine Antibodies." *BioTechniques* 44: 927–929.
- Chowdhury, S. G., R. Ray, D. Bhattacharya, and P. Karmakar. 2022. "DNA Damage Induced Cellular Senescence and Its PTEN-Armed Exosomes—The Warriors Against Prostate Carcinoma Cells." *Medical Oncology* 39: 34.
- Chu, F. Y., S. C. Haley, and A. Zidovska. 2017. "On the Origin of Shape Fluctuations of the Cell Nucleus." *Proceedings of the National Academy of Sciences of the United States of America* 114: 10338–10343.
- Chytilova, E., J. Macas, E. Sliwinska, S. M. Rafelski, G. M. Lambert, and D. W. Galbraith. 2000. "Nuclear Dynamics in *Arabidopsis thaliana*." *Molecular Biology of the Cell* 11: 2733–2741.
- Desvoyes, B., A. Arana-Echarri, M. D. Barea, and C. Gutierrez. 2020. "A Comprehensive Fluorescent Sensor for Spatiotemporal Cell Cycle Analysis in Arabidopsis." *Nature Plants* 6: 1330–1334.
- Echevarria, C., B. Desvoyes, and M. Marconi, et al. 2022. "Stem Cell Regulators Control a G1 Duration Gradient in the Plant Root Meristem." bioRxiv.
- Echevarria, C., C. Gutierrez, and B. Desvoyes. 2021. "Tools for Assessing Cell-Cycle Progression in Plants." *Plant & Cell Physiology* 62: 1231–1238.
- Efremov, A. K., L. Hovan, and J. Yan. 2022. "Nucleus Size and Its Effect on Nucleosome Stability in Living Cells." *Biophysical Journal* 121: 4189–4204.
- Eschweiler D. Smith R.S. Stegmaier J. 2022 Robust 3D Cell Segmentation: Extending the View of Cellpose. In Proceedings - International Conference on Image Processing, ICIP
- Fridman, Y., S. Strauss, G. Horev, et al. 2021. "The Root Meristem Is Shaped by Brassinosteroid Control of Cell Geometry." *Nature Plants* 7, no. 11: 1475–1484. <https://doi.org/10.1038/s41477-021-01014-9>.
- Goldy, C., J. A. Pedroza-Garcia, N. Breakfield, et al. 2021. "The Arabidopsis GRAS-Type SCL28 Transcription Factor Controls the Mitotic Cell Cycle and Division Plane Orientation." *Proceedings of the National Academy of Sciences of the United States of America* 118: e2005256118.
- Goto, C., I. Hara-Nishimura, and K. Tamura. 2021. "Regulation and Physiological Significance of the Nuclear Shape in Plants." *Frontiers in Plant Science* 12: 673905.
- Grootjans, S., B. Hassannia, I. Delrue, et al. 2016. "A Real-Time Fluorometric Method for the Simultaneous Detection of Cell Death Type and Rate." *Nature Protocols* 11: 1444–1454.
- Hayashi, K., J. Hasegawa, and S. Matsunaga. 2013. "The Boundary of the Meristematic and Elongation Zones in Roots: Endoreduplication Precedes Rapid Cell Expansion." *Scientific Reports* 3, no. 1: 2723. <https://doi.org/10.1038/srep02723>.
- Helariutta, Y., H. Fukaki, J. Wysocka-Diller, et al. 2000. "The SHORT-ROOT Gene Controls Radial Patterning of the Arabidopsis Root Through Radial Signaling." *Cell* 101: 555–567.
- Imoto, A., M. Yamada, T. Sakamoto, et al. 2021. "A Clearsee-Based Clearing Protocol for 3D Visualization of Arabidopsis Thaliana Embryos." *Plants* 10: 190.
- Karg, T. J., and K. G. Golic. 2018. "Photoconversion of DAPI and Hoechst Dyes to Green and Red-Emitting Forms After Exposure to UV Excitation." *Chromosoma* 127: 235–245.
- Kerstens, M., S. Strauss, R. Smith, and V. Willemsen. 2020. "From Stained Plant Tissues to Quantitative Cell Segmentation Analysis With MorphoGraphX." In *Methods in Molecular Biology*.
- Kotogány, E., D. Dudits, G. V. Horváth, and F. Ayaydin. 2010. "A Rapid and Robust Assay for Detection of S-Phase Cell Cycle Progression in Plant Cells and Tissues by Using Ethynyl Deoxyuridine." *Plant Methods* 6, no. 1: 5. <https://doi.org/10.1186/1746-4811-6-5>.
- Kurihara, D., Y. Mizuta, Y. Sato, and T. Higashiyama. 2015. "ClearSee: A Rapid Optical Clearing Reagent for Whole-Plant Fluorescence Imaging." *Development (Cambridge)* 142: 4168–4179.
- Lasok, H., H. Nziengui, P. Kochersperger, and F. A. Ditengou. 2023. "Arabidopsis Root Development Regulation by the Endogenous Folate Precursor, Para-Aminobenzoic Acid, via Modulation of the Root Cell Cycle." *Plants* 12: 4076.
- Lavrekha, V. V., T. Pasternak, V. B. Ivanov, K. Palme, and V. V. Mironova. 2017. "3D Analysis of Mitosis Distribution Highlights the Longitudinal Zonation and Diarch Symmetry in Proliferation Activity of the Arabidopsis Thaliana Root Meristem." *Plant Journal* 92: 834–845.
- Liu, K., T. Schmidt, T. Blein, J. Durr, K. Palme, and O. Ronneberger. 2013. "Joint 3D Cell Segmentation and Classification in the Arabidopsis Root Using Energy Minimization and Shape Priors." In *Proceedings - International Symposium on Biomedical Imaging*.
- Mathur, J., S. Griffiths, K. Barton, and M. H. Schattat. 2012. "Green-to-Red Photoconvertible mEosFP-Aided Live Imaging in Plants." In *Methods in Enzymology*, vol. 504, 163–181.
- Montenegro-Johnson, T., S. Strauss, M. D. B. Jackson, L. Walker, R. S. Smith, and G. W. Bassel. 2019. "3DCellAtlas Meristem: A Tool for the Global Cellular Annotation of Shoot Apical Meristems." *Plant Methods* 15: 33.
- Musielak, T., P. Bürgel, M. Kolb, and M. Bayer. 2016. "Use of SCRI Renaissance 2200 (SR2200) as a Versatile Dye for Imaging of Developing Embryos, Whole Ovules, Pollen Tubes and Roots." *Bio-Protocol* 6: e1935.
- Musielak, T., L. Schenkel, M. Kolb, A. Henschen, and M. Bayer. 2015. "A Simple and Versatile Cell Wall Staining Protocol to Study Plant Reproduction." *Plant Reproduction* 28: 161–169.
- Nakayama, H., K. Kawade, H. Tsukaya, and S. Kimura. 2015. "Detection of the Cell Proliferation Zone in Leaves by Using EdU." *Bio-Protocol* 5: e1600.
- Pasternak, T., T. Falk, and A. I. Paponov. 2021. "Deep-Resolution Plant Phenotyping Platform Description. v1." protocols.io. Accessed January 31, 2025. <https://doi.org/10.17504/protocols.io.br5dm6a6>.
- Pasternak, T., T. Haser, T. Falk, O. Ronneberger, K. Palme, and L. Otten. 2017. "A 3D Digital Atlas of the *Nicotiana tabacum* Root Tip and Its Use to Investigate Changes in the Root Apical Meristem Induced by the Agrobacterium 6B Oncogene." *Plant Journal* 92: 31–42.
- Pasternak, T., S. Kircher, and K. Palme. 2021. "Estimation of Cell Cycle Kinetics in Higher Plant Root Meristem Links Organ Position With Cellular Fate and Chromatin Structure." bioRxiv.

Pasternak, T., S. Kircher, J. M. Pérez-Pérez, and K. Palme. 2022. “A Simple Pipeline for Cell Cycle Kinetic Studies in the Root Apical Meristem.” *Journal of Experimental Botany* 73: 4683–4695.

Pasternak, T., and J. M. Pérez-Pérez. 2021. “Methods of In Situ Quantitative Root Biology.” *Plants* 10: 2399.

Pasternak, T., O. Tietz, K. Rapp, et al. 2015. “Protocol: An Improved and Universal Procedure for Whole-Mount Immunolocalization in Plants.” *Plant Methods* 11: 50.

Reyes-Olalde, J. I., and S. de Folter. 2019. “Control of Stem Cell Activity in the Carpel Margin Meristem (CMM) in Arabidopsis.” *Plant Reproduction* 32: 123–136.

Romero-Arias, J. R., V. Hernández-Hernández, M. Benítez, E. R. Alvarez-Buylla, and R. A. Barrio. 2017. “Model of Polar Auxin Transport Coupled to Mechanical Forces Retrieves Robust Morphogenesis Along the Arabidopsis Root.” *Physical Review E* 95: 032410.

Sarkar, R., D. Darby, S. Meilhac, and J.-C. Olivo-Marin. 2022. “3D Cell Morphology Detection by Association for Embryo Heart Morphogenesis.” *Biological Imaging* 2: e2.

Savina, M. S., T. Pasternak, N. A. Omelyanchuk, et al. 2020. “Cell Dynamics in WOX5-Overexpressing Root Tips: The Impact of Local Auxin Biosynthesis.” *Frontiers in Plant Science* 11: 560169.

Schmidt, T., T. Pasternak, K. Liu, et al. 2014. “The iRoCS Toolbox - 3D Analysis of the Plant Root Apical Meristem at Cellular Resolution.” *Plant Journal* 77: 806–814.

Sclafani, R. A., and T. M. Holzen. 2007. “Cell Cycle Regulation of DNA Replication.” *Annual Review of Genetics* 41: 237–280.

Strauss, S., A. Runions, B. Lane, et al. 2022. “Using Positional Information to Provide Context for Biological Image Analysis With MorphoGraphX 2.0.” *eLife* 11: e72601.

Stringer, C., T. Wang, M. Michaelos, and M. Pachitariu. 2021. “Cellpose: A Generalist Algorithm for Cellular Segmentation.” *Nature Methods* 18: 100–106.

Truernit, E., and J. Haseloff. 2008. “A Simple Way to Identify Non-Viable Cells Within Living Plant Tissue Using Confocal Microscopy.” *Plant Methods* 4: 15.

Ursache, R., T. G. Andersen, P. Marhavý, and N. Geldner. 2018. “A Protocol for Combining Fluorescent Proteins With Histological Stains for Diverse Cell Wall Components.” *Plant Journal* 93: 399–412.

Velappan, Y., S. Signorelli, and M. J. Considine. 2017. “Cell Cycle Arrest in Plants: What Distinguishes Quiescence, Dormancy and Differentiated G1?” *Annals of Botany* 120, no. 4: 495–509. <https://doi.org/10.1093/aob/mcx082>.

Vijayan, A., T. A. Mody, Q. Yu, et al. 2024. “A Deep Learning-Based Toolkit for 3D Nuclei Segmentation and Quantitative Analysis in Cellular and Tissue Context.” *Development* 151: 14.

Warner, C. A., M. L. Biedrzycki, S. S. Jacobs, R. J. Wisser, J. L. Caplan, and D. J. Sherrier. 2014. “An Optical Clearing Technique for Plant Tissues Allowing Deep Imaging and Compatible With Fluorescence Microscopy.” *Plant Physiology* 166: 1684–1687.

Wolny, A., L. Cerrone, A. Vijayan, et al. 2020. “Accurate and Versatile 3D Segmentation of Plant Tissues at Cellular Resolution.” *eLife* 9: e57613.

Yin, K., M. Ueda, H. Takagi, et al. 2014. “A Dual-Color Marker System for In Vivo Visualization of Cell Cycle Progression in Arabidopsis.” *Plant Journal* 80: 541–552.

Murashige, T., and F. Skoog. 1962. “A Revised Medium for Rapid Growth and Bio Assays With Tobacco Tissue Cultures.” *Physiologia Plantarum* 15, no. 3: 473–497. <https://doi.org/10.1111/j.1399-3054.1962.tb08052.x>.

Tapia-López, R., B. García-Ponce, J. G. Dubrovsky, et al. 2008. “An AGAMOUS-Related MADS-Box Gene, XAL1 (AGL12), Regulates Root Meristem Cell Proliferation and Flowering Transition in Arabidopsis.”

Plant Physiology 146, no. 3: 1182–1192. <https://doi.org/10.1104/pp.107.108647>.

Supporting Information

Additional supporting information can be found online in the Supporting Information section.